



Contents lists available at ScienceDirect

Applied Geochemistry

journal homepage: [www.elsevier.com/locate/apgeochem](http://www.elsevier.com/locate/apgeochem)

## Chemical evolution of the Mt. Hekla, Iceland, groundwaters: A natural analogue for CO<sub>2</sub> sequestration in basaltic rocks

Therese K. Flaathen<sup>a,b,c,\*</sup>, Sigurður R. Gislason<sup>d</sup>, Eric H. Oelkers<sup>a,b,c</sup>, Árný E. Sveinbjörnsdóttir<sup>d</sup>

<sup>a</sup> Université de Toulouse; UPS (OMP); LMTG; 14 Avenue Edouard Belin, F-31400 Toulouse, France

<sup>b</sup> CNRS; LMTG; F-31400 Toulouse, France

<sup>c</sup> IRD; LMTG; F-31400 Toulouse, France

<sup>d</sup> Institute of Earth Sciences, University of Iceland, Sturlugata 7, 101 Reykjavík, Iceland

### ARTICLE INFO

#### Article history:

Received 11 July 2008

Accepted 18 December 2008

Available online xxxxx

Editorial Handling by Dr. R. Fuge

### ABSTRACT

A detailed study of the chemical composition of the groundwater surrounding the Mt. Hekla volcano in south Iceland was performed to assess fluid evolution and toxic metal mobility during CO<sub>2</sub>-rich fluid–basalt interaction. These fluids provide a natural analogue for evaluating the consequences of CO<sub>2</sub> sequestration in basalt. The concentration of dissolved inorganic C in these groundwaters decreases from 3.88 to 0.746 mmol/kg with increasing basalt dissolution while the pH increases from 6.9 to 9.2. This observation provides direct evidence of the potential for basalt dissolution to sequester CO<sub>2</sub>. Reaction path calculations suggest that dolomite and calcite precipitation is largely responsible for this drop in groundwater dissolved C concentration. The concentrations of toxic metal(loid)s in the waters are low, for example the maximum measured concentrations of Cd, As and Pb were 0.09, 22.8 and 0.06 nmol/kg, respectively. Reaction path modelling indicates that although many toxic metals may be initially liberated by the dissolution of basalt by acidic CO<sub>2</sub>-rich solutions, these metals are reincorporated into solid phases as the groundwaters are neutralized by continued basalt dissolution. The identity of the secondary toxic metal bearing phases depends on the metal. For example, calculations suggest that Sr and Ba are incorporated into carbonates, while Pb, Zn and Cd are incorporated into Fe (oxy)hydroxide phases.

© 2008 Elsevier Ltd. All rights reserved.

### 1. Introduction

A large current effort is being made to identify and optimize CO<sub>2</sub> sequestration technologies to address the potential dangers associated with increased atmospheric CO<sub>2</sub> content (IPCC, 2005; Oelkers and Schott, 2005; Oelkers and Cole, 2008). One such technology involves the injection of CO<sub>2</sub> into basaltic rocks (McGrail et al., 2006; Gislason et al., 2007; Matter et al., 2007; Oelkers et al., 2008). This method offers several potential advantages including the availability of divalent metal cations such as Ca<sup>2+</sup> and Mg<sup>2+</sup> which could provoke the precipitation of stable carbonate minerals (Walker and Hays, 1981; Gaillardet et al., 1999; Brady and Gislason, 1997; Wolff-Boenisch et al., 2006). One method to assess both the potential and the risks associated with CO<sub>2</sub> sequestration in basaltic rocks is through the study of natural analogues. One such analogue is the Mt. Hekla groundwater system. The groundwaters surrounding Mt. Hekla experience large inputs of magmatic gases dominated by CO<sub>2</sub> (Kjartansson, 1957; Gislason et al., 1992; Flaathen and Gislason, 2007). A study of the chemical composition of these groundwaters should, therefore, provide insight into the fate

and consequences of injecting CO<sub>2</sub> into basaltic rocks. Taking advantage of this natural analogue, waters have been regularly sampled from 26 springs surrounding Mt. Hekla. Analyses of these waters, together with reaction path modelling, suggest that (1) CO<sub>2</sub> is readily sequestered, via fluid–basalt interaction through carbonate mineral precipitation and (2) although they may be liberated due to basalt dissolution, toxic metals are readily reincorporated into solid phases as the basalt neutralizes the initially CO<sub>2</sub>-rich fluid. The purpose of this paper is to present the results of this combined field and modelling study providing insight into the consequences of injecting CO<sub>2</sub> into basaltic rocks.

### 2. Geological background: Hekla volcano and its groundwater system

The Mt. Hekla volcano (63.98°N, 19.70°W) is a ridge built up by repeated fissure eruptions. The volcano strikes N 65°E and is located where the eastern volcanic zone, meets the South Iceland seismic zone (Gudmundsson et al., 1992). It is one of Europe's most active volcanoes with 18 eruptions during the last 900 a (Gronvold et al., 1983). The most recent eruptions occurred during 1970, 1980, 1991 and 2000. The bulk of the erupted material during the last 900 a is of basaltic andesite composition (Sigvaldason, 1974; Gudmundsson et al. 1992; Moune et al., 2006). The main

\* Corresponding author. Address: Université de Toulouse; UPS (OMP); LMTG; 14 Avenue Edouard Belin, F-31400 Toulouse, France. Fax: +33 0 5 61 33 25 60.  
E-mail addresses: [flaathen@gmail.com](mailto:flaathen@gmail.com), [therese@hi.is](mailto:therese@hi.is) (T.K. Flaathen).

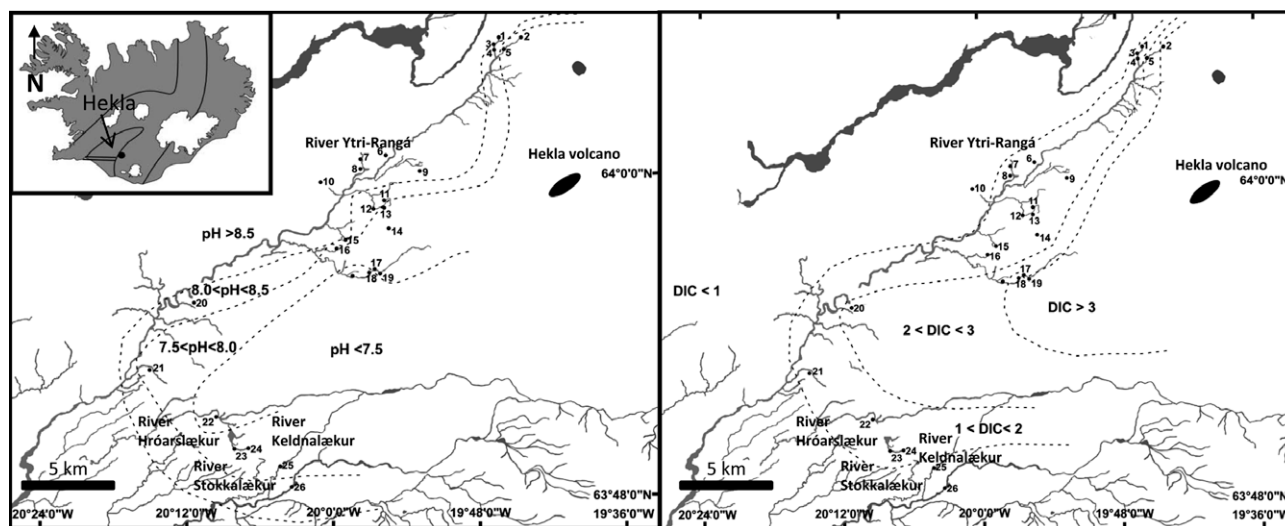


Fig. 1. Map showing the location of the Hekla volcano, the main springs, and the sample sites. Superimposed on the map is a) *in situ* pH in the spring water samples, and b) the dissolved inorganic C (DIC) concentration (meq/L) in the spring water samples.

rock forming phases of the basaltic andesitic tephra are glass (97.9%), plagioclase (1.6%), magnetite (0.2%), olivine (0.2%) and pyroxene (0.1%) (Sigvaldason, 1974). The basaltic andesite lava flows consist of dense dark rocks with relatively high viscosity upon extrusion, forming an aa or block type lava. Phenocrysts are rare in the 1970 lava flows (Sigvaldason, 1974).

The groundwater in the Mt. Hekla region flows from the NE to the SW along the volcanic zone. Groundwater discharge is observed at the source of the Ytri-Rangá River, NW of the volcano, as well as at springs west, south and SE of the volcano (Árnason, 1976). The surface hydrology of this system can be seen in Fig. 1. The post-glacial lava flows (<10 ka) and volcanic ash fallouts are very porous, preventing surface runoff in the vicinity of the volcano.

The groundwater chemistry of the Mt. Hekla system is strongly influenced by the input of magmatic gases and it is known for CO<sub>2</sub> degassing during eruptions (Kjartansson, 1957; Gislason et al., 1992; Flaathen and Gislason, 2007). During its 1947 eruption, several animals, birds, and sheep, were found suffocated due to high CO<sub>2</sub> concentrations in shallow depressions in the lava fields. Formation of Ca and Mg carbonates in discharging groundwater has been observed in the area (Kjartansson, 1957). The long-term influx of magmatic gases from the magma chamber and their interaction with basalt through the aqueous phase has led to elevated concentrations of total dissolved solids (TDS) and high alkalinity in the Hekla groundwater (Gislason et al., 1992).

### 3. Materials and methods

#### 3.1. Water samples from springs

A total of 111 samples from 26 springs surrounding Mt. Hekla were collected during 1988, 1991, 1992 and 2006. The locations of the sampling sites are shown in Fig. 1. Each spring was collected for 1–6 times except spring 18, which was sampled 19 times. The samples were taken during all seasons. The water samples were filtered immediately after sampling through 0.2 µm Millipore cellulose acetate membranes into high density polyethylene bottles. Samples taken for pH and dissolved inorganic C (DIC) measurement were collected in brown glass bottles with a special cap designed to eliminate air inside the bottles. Samples intended for major and trace element analyses were acidified using concen-

trated suprapur HNO<sub>3</sub>. Alkalinity/dissolved inorganic C and pH were determined in the laboratory at ambient temperature 1–5 days after sampling.

Samples collected during 1988–1992 were analyzed at the University of Iceland. Fluorine and Cl were measured with ion-selective electrodes. Silica, Na, K, Ca, Mg, S, Fe, Mn, Ti, Al and Sr were measured by inductively coupled plasma atomic emission spectroscopy (ICP–AES). The detection limit for these analyses were  $2.5 \times 10^{-8}$ ,  $2.1 \times 10^{-7}$ ,  $4.3 \times 10^{-7}$ ,  $1.3 \times 10^{-5}$ ,  $3.6 \times 10^{-6}$ ,  $3.7 \times 10^{-7}$ ,  $3.6 \times 10^{-7}$ ,  $9.3 \times 10^{-7}$ ,  $2.3 \times 10^{-8}$  and  $1.0 \times 10^{-5}$  mol/kg, for Ca, Mg, Na, K, Si, Al, Fe, B, Sr and SO<sub>4</sub><sup>2-</sup>, respectively. The uncertainty of these analyses was 3–5%.

For samples collected in 2006, F<sup>-</sup>, Cl<sup>-</sup> and SO<sub>4</sub><sup>2-</sup> were measured by ion-chromatography (IC) at the Institute of Earth Sciences, University of Iceland; these results have an uncertainty of 3–5% and the detection limit was  $3.68 \times 10^{-7}$ ,  $6.35 \times 10^{-6}$  and  $3.12 \times 10^{-7}$  mol/kg, respectively. The cations, other than Fe, were analyzed at Analytica-SCAB, Luleå, Sweden. Calcium, K, Mg, Na, Si, Sr and V were measured with ICP–AES and Al, Ba, Cd, Co, Cr, Cu, Mn, Mo, Ni, total P, Pb and Zn together with As, B, Li, Ti and the lanthanides were measured using inductively coupled plasma field mass spectroscopy (ICP–SFMS). Mercury and Se were measured using atomic fluorescence spectroscopy (AFS). The detection limits for these latter analyses were  $2.5 \times 10^{-6}$ ,  $3.7 \times 10^{-6}$ ,  $4.3 \times 10^{-6}$ ,  $1.0 \times 10^{-5}$ ,  $1.0 \times 10^{-6}$  and  $7.4 \times 10^{-9}$  mol/kg for Ca, Mg, Na, K, Si and Al, respectively. The detection limits for the trace elements, Ba, Cd, Co, Cu, Mn, Pb, Sr and Zn, were  $7.3 \times 10^{-11}$ ,  $1.8 \times 10^{-11}$ ,  $3.4 \times 10^{-11}$ ,  $1.6 \times 10^{-9}$ ,  $5.5 \times 10^{-10}$ ,  $4.8 \times 10^{-11}$ ,  $2.3 \times 10^{-8}$  and  $3.1 \times 10^{-9}$  mol/kg, respectively. Iron was analyzed at Mátis, Iceland by ICP–MS, with a detection limit of  $4.5 \times 10^{-9}$  mol/kg. The measurements of these major elements together with Sr, P, Ba, Mo and V have an uncertainty between 12% and 15%. The uncertainty for the elements Al, Cr, Cu and Li varies between 15% and 25%, while the uncertainty of the other measured trace metals varies between 30% and 160%.

#### 3.2. Thermodynamic calculations and reaction path modelling

##### 3.2.1. Speciation and saturation state calculations

Speciation and saturation-state calculations were performed using the PHREEQC 2.14.2 computer code (Parkhurst and Appelo, 1999). The database lnl (The database used in the present study

**Table 1**

Secondary minerals assumed to precipitate during the reaction path modelling performed in the present study.

Mineral name	Formula
Calcite	CaCO <sub>3</sub>
Cerussite	PbCO <sub>3</sub>
Chalcedony	SiO <sub>2</sub>
Clinocllore-14A	Mg <sub>5</sub> Al <sub>2</sub> Si <sub>3</sub> O <sub>10</sub> (OH) <sub>8</sub>
Delafossite	CuFe <sub>2</sub> O <sub>4</sub>
Ferrite-Zn	ZnFe <sub>2</sub> O <sub>4</sub>
Hematite	Fe <sub>2</sub> O <sub>3</sub>
Heulandite	Ba <sub>0.65</sub> Sr <sub>0.175</sub> Ca <sub>0.585</sub> K <sub>0.132</sub> Na <sub>0.383</sub> Al <sub>2.165</sub> Si <sub>6.835</sub> O <sub>18</sub> ·6H <sub>2</sub> O
Hydrozincite	Zn <sub>5</sub> (OH) <sub>6</sub> (CO <sub>3</sub> ) <sub>2</sub>
Kaolinite	Al <sub>2</sub> Si <sub>2</sub> O <sub>5</sub> (OH) <sub>4</sub>
Laumontite	CaAl <sub>2</sub> Si <sub>4</sub> O <sub>12</sub> ·4H <sub>2</sub> O
Magnesite	MgCO <sub>3</sub>
Manganite	MnO(OH)
Otavite	CdCO <sub>3</sub>
Rhodochrosite	MnCO <sub>3</sub>
Siderite	FeCO <sub>3</sub>
Smectite-high-Fe-Mg	Ca <sub>0.025</sub> Na <sub>0.1</sub> K <sub>0.2</sub> Fe <sub>0.7</sub> Mg <sub>1.15</sub> Al <sub>1.25</sub> Si <sub>3.5</sub> O <sub>10</sub> (OH) <sub>2</sub>
Smectite-low-Fe-Mg	Ca <sub>0.02</sub> Na <sub>0.15</sub> K <sub>0.2</sub> Fe <sub>0.45</sub> Mg <sub>0.9</sub> Al <sub>1.25</sub> Si <sub>3.75</sub> O <sub>10</sub> (OH) <sub>12</sub>
Smithsonite	ZnCO <sub>3</sub>
Sphaerocobaltite	CoCO <sub>3</sub>
Strontianite	SrCO <sub>3</sub>
Witherite	BaCO <sub>3</sub>

has the id: lnl.dat 85 2005-02-02. The data for this database were taken from 'thermo.com.V8.R6.230' prepared by Jim Johnson at Lawrence Livermore National Laboratory.) was used other than for the thermodynamic data for hydrated basaltic andesitic Hekla 2000 glass, which was taken from Wolff-Boenisch et al. (2004). The saturation state of the fluid is quantified in terms of the Gibbs free energy of reaction,  $\Delta G_r$ , of the dissolving minerals or glass (Gislason and Arnórsson, 1990, 1993). The Gibbs free energy of reaction is equal to zero at equilibrium. If  $\Delta G_r < 0$ , the mineral is undersaturated. Dissolution rate equations for minerals and glasses are commonly written in terms of the  $\Delta G_r$  (e.g. Gislason and Oelkers 2003).

### 3.2.2. Reaction path modelling

Reaction path modelling was performed to investigate the fate of metals and dissolved C in the Hekla groundwater using PHREEQC 2.14.2 and assuming the groundwater system is closed with respect to both CO<sub>2</sub> and secondary minerals. This modelling involves the dissolution of Hekla andesitic basalt (Moune et al., 2006) into CO<sub>2</sub>-rich groundwater. The chemical composition of the Hekla lava has been constant during the last four eruptions (Gudmundsson et al., 1992; Moune et al., 2006). The 2000 lava has a chemical formula normalized to one Si consistent with Si P<sub>0.01</sub> Ti<sub>0.03</sub> Al<sub>0.31</sub> Fe<sub>0.17</sub>

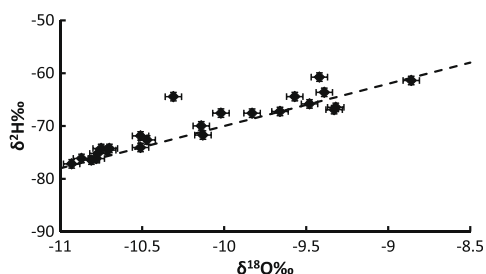


**Fig. 2.**  $\delta^{18}\text{O}$  versus  $\delta^2\text{H}$  values in the spring waters. The symbols represent the spring water samples and the line represents the meteoric water line (Craig, 1961). The coherence between the symbols and the line indicates a meteoric origin of the waters.

Mg<sub>0.08</sub> Mn<sub>0.005</sub> Ca<sub>0.13</sub> Na<sub>0.16</sub> K<sub>0.03</sub> O<sub>3.13</sub>. The concentration of the trace metals, Ba, Cd, Co, Cu, Sr, Pb and Zn, are  $2.50 \times 10^{-3}$ ,  $1.65 \times 10^{-6}$ ,  $7.86 \times 10^{-4}$ ,  $4.12 \times 10^{-4}$ ,  $4.58 \times 10^{-3}$ ,  $1.57 \times 10^{-5}$  and  $3.23 \times 10^{-3}$  mol/kg, respectively (Moune et al., 2006). The different constituents of the Hekla glass were added to the reaction fluid in the reaction path calculations as oxides and were forced to react with the solution in proportion to their composition in the glass. The temperature of the model was kept constant at 3.7 °C consistent with the average temperature of local groundwaters.

### 3.2.3. Initial modelling conditions and secondary mineral formation

The initial solution for the reaction path modelling performed in this study had the chemical composition of melted snow from SW Iceland (Gislason et al., 2000) equilibrated with 0.05 bar CO<sub>2</sub>; this CO<sub>2</sub> pressure is 130 times that of the atmosphere. The resulting solution has a pH of 4.5. This CO<sub>2</sub> concentration was chosen to be consistent with the measured groundwater compositions such that the final Na concentration of the reaction path model matched that of the Na in the springs (see Fig. 8 below). The total aqueous concentration of Na was used for this purpose because it is negligibly incorporated into secondary phases during low temperature basalt alteration (Gislason et al., 1996); this choice is confirmed by the correspondence of measured fluid compositions with the model results presented below. Based on this concentration the total amount of solid, reactant was calculated to be 0.0098 mol of basaltic glass per kg of water to attain a final pH of 9.4.

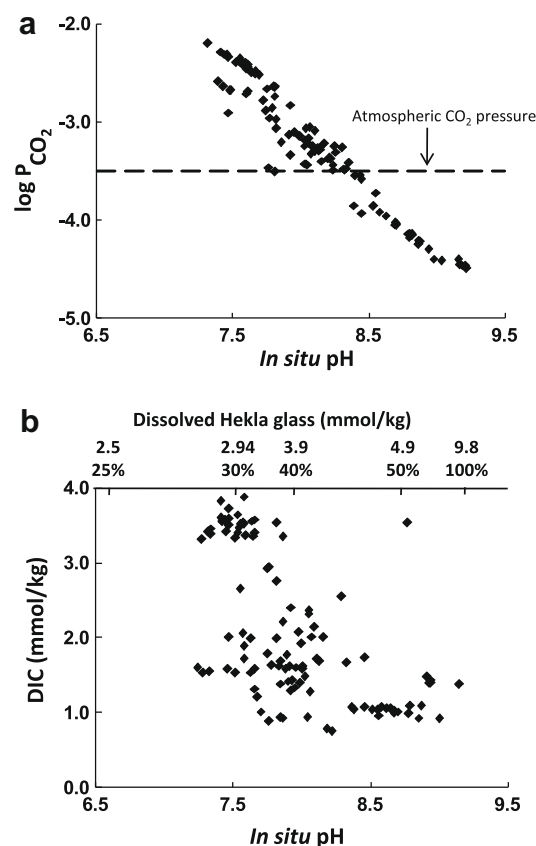


**Fig. 3.** (a) The symbols represent the partial pressure of CO<sub>2</sub> calculated using PHREEQC 2.14.2 in the springs plotted versus pH at the measured spring water temperature at the time of sampling (*in situ* pH). The stippled line is the atmospheric partial pressure of CO<sub>2</sub>. The uncertainty of the measurements is approximated by the symbol size. (b) DIC concentrations in the spring water samples plotted versus *in situ* pH. The secondary x-axis shows the amount of Hekla glass dissolved in model calculation to reach the pH.

When Mt. Hekla andesitic basaltic volcanic glass dissolves in the initial CO<sub>2</sub>-rich solution, the concentration of aqueous species increases and it eventually becomes supersaturated with respect to secondary minerals. The secondary minerals allowed to precipitate in the model calculations are those that are common in low-temperature alteration of basalt in Iceland (Mehegan et al., 1982; Kristmannsdóttir, 1982; Gislason et al., 1993; Neuhoff et al., 1999).

A list of all secondary phases used in the model calculations are to be found in Table 1. Note that although allophane is a common clay mineral found in Iceland, it is not considered as a secondary phase in these calculations because this mineral is not in the *lInl.dat* database. Kaolinite is taken as a proxy for allophane in the calculations. In the same way, oxides and multiple oxide minerals such as hematite, delafossite, CoFe<sub>2</sub>O<sub>4</sub> and ZnFe<sub>2</sub>O<sub>4</sub> are essentially proxies

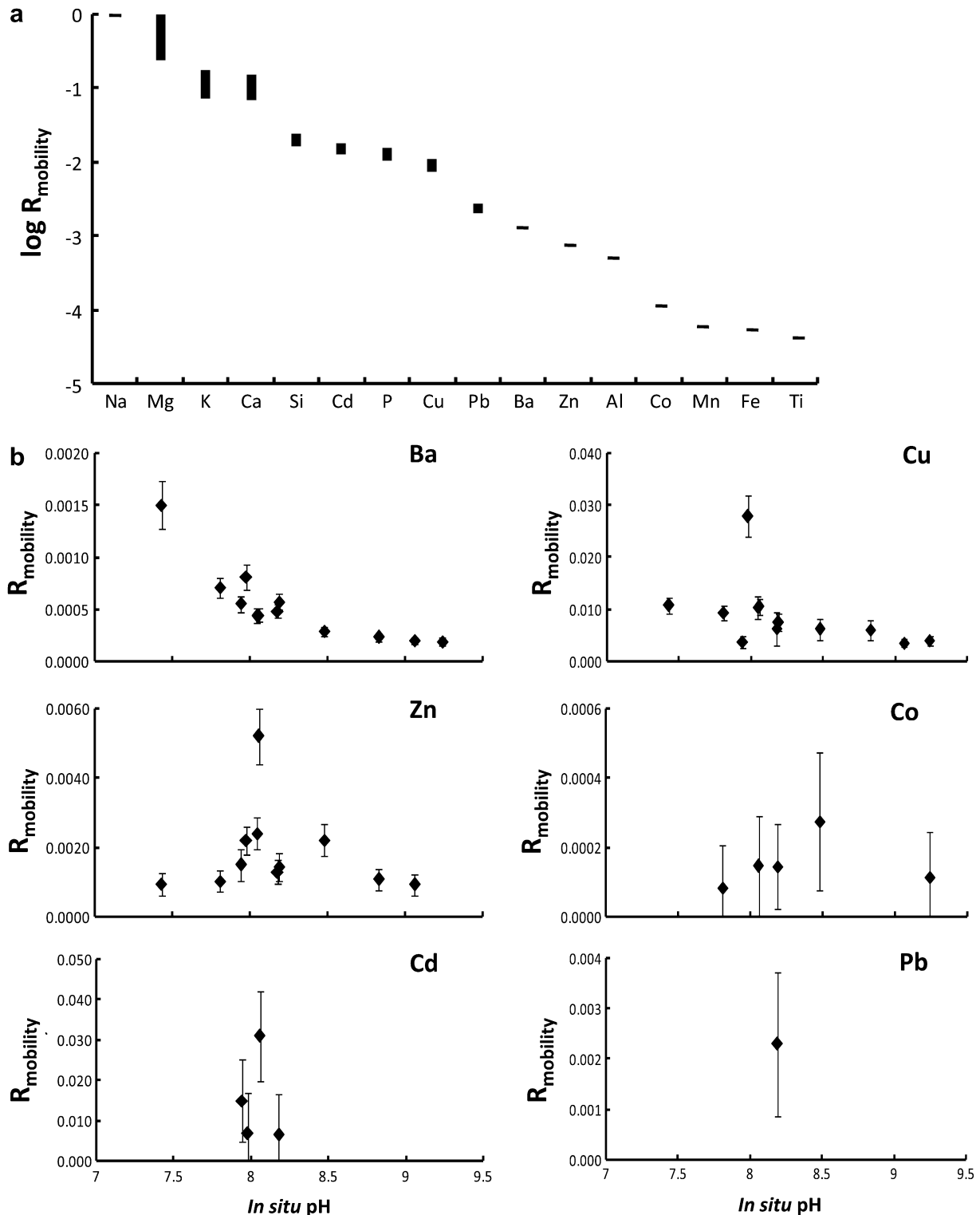


Fig. 4. (a) The logarithm of the relative mobility of major and trace elements in the spring waters. The concentration of Fe, Al, Mn, Cd, Co, Pb and Zn were in some samples below detection limit. (b) The mobility of the trace metals in the Hekla groundwater versus pH (see text).

**Table 2**

The annual discharge, DIC concentration and CO<sub>2</sub> flux in the rivers from the Hekla groundwater system.

Rivers	Annual discharge <sup>a</sup> (km <sup>3</sup> /year)	DIC (mmol/kg)	Annual CO <sub>2</sub> flux (ton/year)
Ytri-Ranga	1.33 <sup>b</sup>	1.57	8.89 × 10 <sup>4</sup>
Stokkalaekur	0.256	0.94	7.62 × 10 <sup>3</sup>
Hroarslaekur	0.394	0.94	1.33 × 10 <sup>4</sup>
Keldulaekur	0.429	0.94	1.48 × 10 <sup>4</sup>
Total	2.409		1.25 × 10 <sup>5</sup>

<sup>a</sup> The discharge of Stokkalaekur, Hroarslaekur and Keldnalaekur was obtained by a single measurement taken on each river on March 14th, 1992.

<sup>b</sup> The discharge of Ytri-Ranga is the mean annual discharge for the years 1996–1998 (Gislason et al., 1993).

for related oxy-hydroxide minerals absent from the database. In addition, due to similar database constraints, the zeolites heulandite and laumontite are considered in the model rather than the commonly found thomsonite and analcime.

## 4. Results

### 4.1. Main hydrogeochemical features

The aqueous concentrations of major elements of all samples can be seen in the Appendix. The pH and alkalinity/dissolved inorganic C (DIC) of these waters range from 7.3 to 9.2 and 0.75 to 3.88 meq/kg, respectively. The spatial distribution of these pH and DIC values are shown in Fig. 1. DIC decreases while pH increases with increased distance from the volcano. Total dissolved solids (TDS) range significantly with the highest concentrations close to the volcano.

$\delta^{18}\text{O}$  and  $\delta^2\text{H}$  were measured in the groundwater samples collected in 1988. The results are plotted in Fig. 2 together with the meteoric water line according to Craig (1961). The uncertainty of the measurements is 0.05‰ and 0.8‰ for  $\delta^{18}\text{O}$  and  $\delta^2\text{H}$ , respectively. The coherence between the symbols and the line in Fig. 2 indicates a meteoric origin of the samples collected in this study. This observation coincides with earlier studies which concluded that all Icelandic ground waters are of meteoric origin (Árnason, 1976). According to Árnason (1976), the isotopically heaviest precipitation in Iceland is found along the southern coast with  $\delta^2\text{H}$  of –50‰ while the isotopically lightest precipitation is in the central highlands at –106‰. Those measured in the Hekla waters analyzed in this study range between –60‰ and –77‰. Consistent with the general Icelandic precipitation trends, the lightest  $\delta^2\text{H}$  waters measured in this study were found in the springs located to NE of the Hekla volcano, (springs 1, 3, 7 and 10) whereas the heaviest  $\delta^2\text{H}$  waters are found in the springs to the south of Hekla (springs 20 and 21).

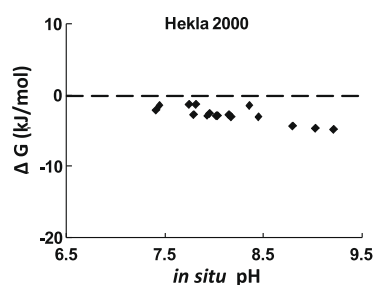


**Fig. 5.** The pH dependence of the saturation state of the hydrated Hekla basaltic andesitic glass, in the sampled spring waters. The symbols represent calculated saturation states and the dashed line shows equilibrium conditions:  $\Delta_r G = 0$ .

The partial pressure of CO<sub>2</sub>,  $P_{\text{CO}_2}$ , of the sampled spring waters is shown as a function of pH in Fig. 3a.  $P_{\text{CO}_2}$  decreases systematically with pH. Carbon dioxide is supersaturated compared to the atmosphere at pH < 8.4 but undersaturated at higher pH. A direct comparison between DIC and pH, is shown Fig. 3b. DIC generally decreases as pH increases. Such a trend is consistent with CO<sub>2</sub> being precipitated as carbonate minerals, such as calcite, from these waters due to its interaction with basalts. Calcite precipitation is also suggested by the saturation state of these spring water samples as reported below.

#### 4.1.1. Mobility of major ions

Bicarbonate is the major anion in the spring water samples with concentrations ranging from 0.0012 to 3.88 mmol/kg. Sulphate and Cl<sup>-</sup> are 1 order and F<sup>-</sup> 2 orders of magnitude less abundant than HCO<sub>3</sub><sup>-</sup>. The most abundant cation is Na<sup>+</sup> with concentrations ranging from 0.42 to 2.50 mmol/kg. Sodium is reported to be the most mobile cation in SW Iceland (Gislason et al., 1996). The relative mobility of an element ( $R_{\text{mobility}}$ ) in the ground water system during basalt weathering can be quantified relative to Na using (Gislason et al., 1996):

$$R_{\text{mobility}} = [X_{\text{water}}/Na_{\text{water}}]/[X_{\text{rock}}/Na_{\text{rock}}] \quad (1)$$

where  $[X_{\text{water}}]$  and  $[Na_{\text{water}}]$  are the average concentrations of the element X, and Na in the springs, and  $[X_{\text{rock}}]$  and  $[Na_{\text{rock}}]$  are the concentrations in the Hekla 2000 lava (Moune et al., 2006). Elemental concentrations were corrected for rainwater input prior to calculating  $R_{\text{mobility}}$  in accord with Gislason et al. (2000). Fig. 4a shows the relative mobility ( $R_{\text{mobility}}$ ) of major and selected trace elements in the springs. The sequence of mobility of the major elements from high to low mobility is Na > Mg > K > Ca > Si > P, which is roughly consistent with those of Gislason et al. (1996), who reported the weathering rates of southern Iceland, and of Aiuppa et al. (2000) who studied the composition of Mt. Etna groundwaters.

#### 4.1.2. Mass flux of carbon

A number of studies have concluded that most of the CO<sub>2</sub> in magma of active volcanoes is lost to non-eruptive degassing (Allard et al., 1991; Aiuppa et al., 2004) and groundwaters (Federico et al., 2002) rather than via eruptive degassing. It seems likely, therefore, that much CO<sub>2</sub> is added to groundwater during dormant periods. To assess the CO<sub>2</sub> flux to groundwater in the dormant Mt. Hekla system, the DIC concentration of sampled springs was used to calculate the CO<sub>2</sub> flux emitted by the Hekla spring water. The studied springs source four rivers, the Ytri-Rangá (Gislason et al., 2003), Stokkalaekur, Hróarslaekur and Keldnalaekur. The location of the rivers can be seen in Fig. 1; their annual discharge is listed in Table 2. The discharge, excluding snow melt events, are stable throughout the year. Gislason et al. (2003) reported 24 discharge measurements of Ytri-Rangá taken at various times throughout one year. The standard deviation of these discharge measurements is 8%. As some of the springs are supersaturated with respect to atmospheric CO<sub>2</sub> some will degas when they arrive at the surface (see Fig. 3). This degassing results in lower DIC concentrations and higher pH of the river samples taken at the discharge measuring station (see Table 2) versus those of the springs.

The annual CO<sub>2</sub> flux of the Mt. Hekla system to the surface can be estimated from the product of spring water DIC concentration and annual mean discharge of the four rivers draining the Mt. Hekla system. The total annual mean discharge of the four rivers draining this system is  $2.41 \times 10^9 \text{ m}^3/\text{a}$ . The DIC concentrations in the springs range from 0.746 to 3.88 mmol/kg, indicating that the annual CO<sub>2</sub> discharge of the Mt Hekla system is between 99,380 and 257,500 ton/a. Note this estimate is based on the assumption that C originating (1) from vegetation and soil and, (2) directly from the atmosphere is negligible. The first assumption is validated by the

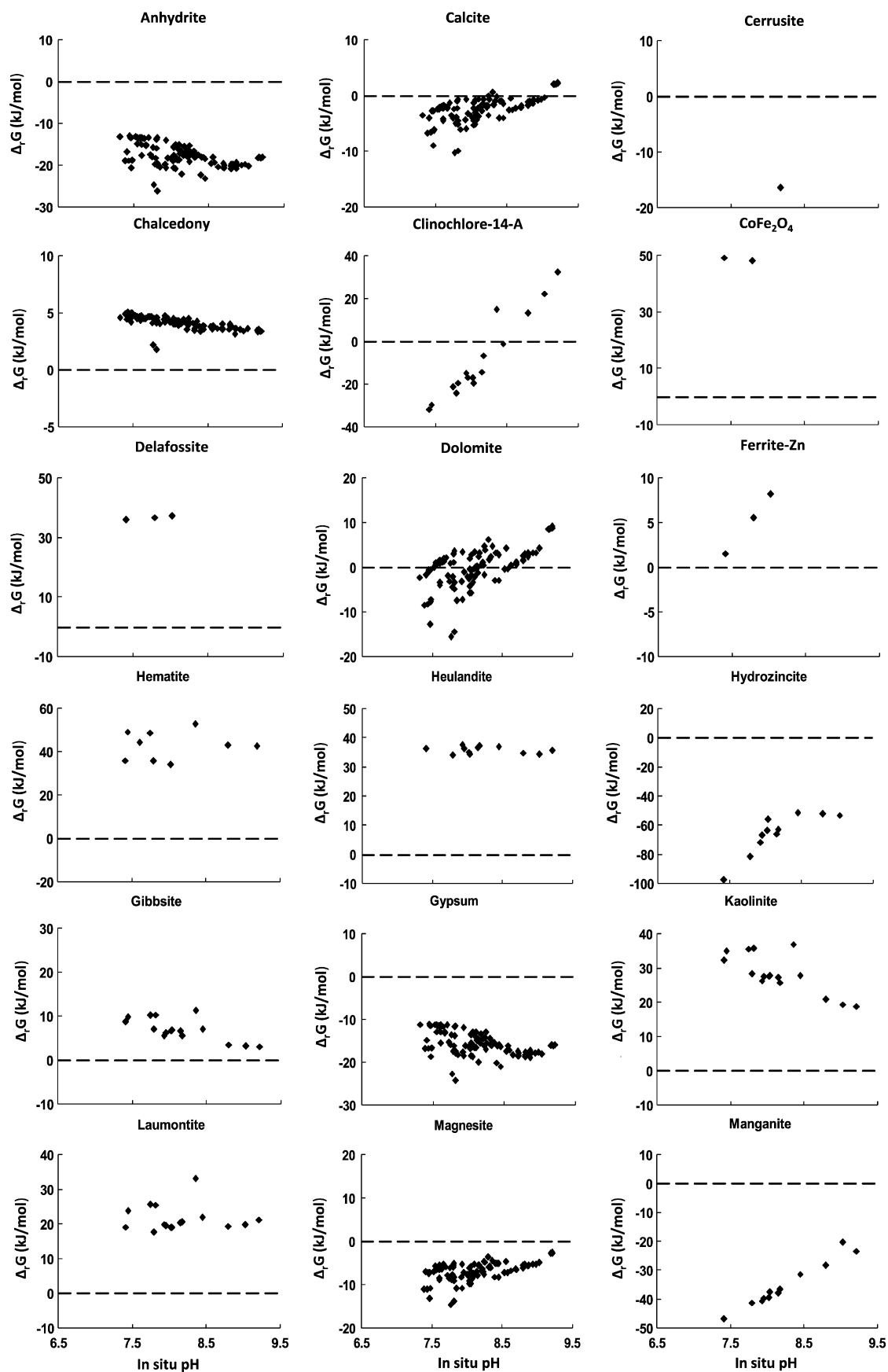


Fig. 6. The pH dependence of the saturation state of secondary minerals in the Hekla spring waters. The symbols represent calculated saturation states and the dashed line corresponds to equilibrium ( $\Delta_1G = 0$ ).

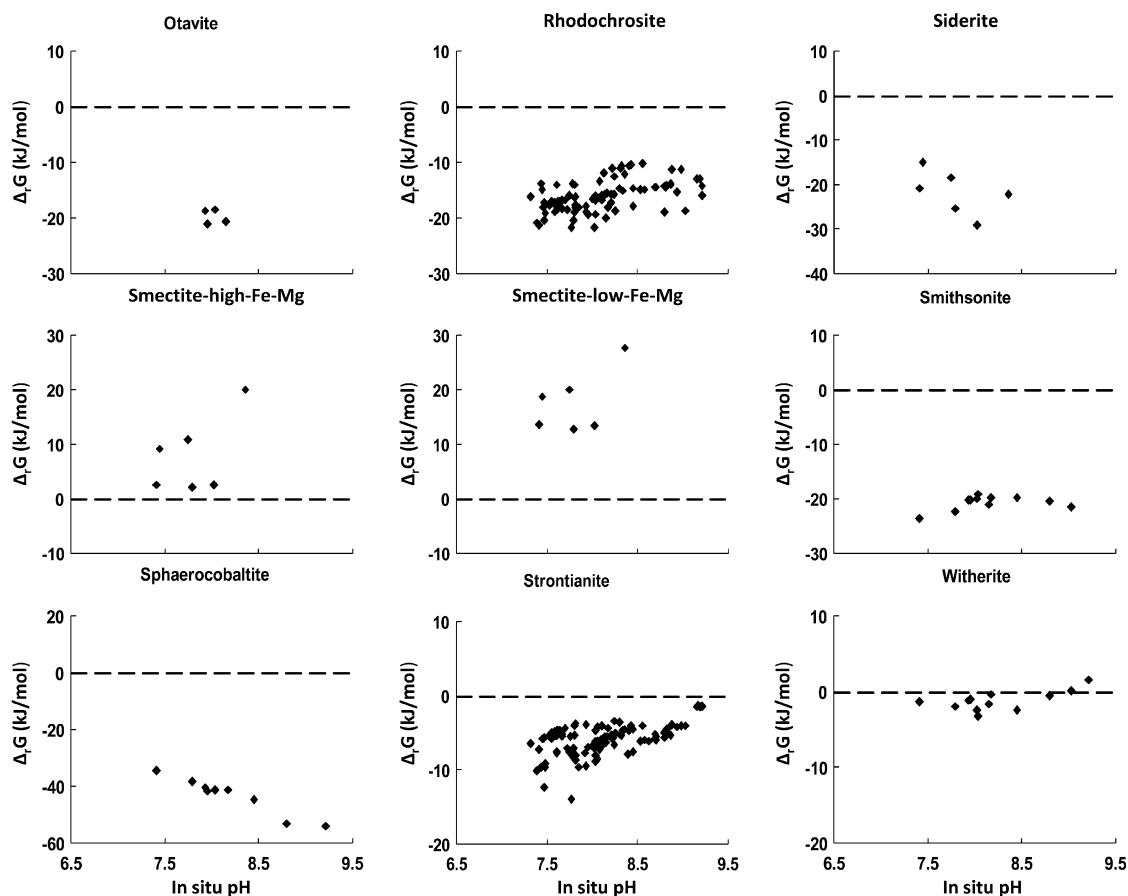


Fig. 6 (continued)

sparse vegetation and soil in the recharge area. The second assumption can be validated by comparing the  $\text{CO}_2$  present in the Mt. Hekla spring waters with that of Icelandic rainwater. The average  $\text{CO}_2$  content of Icelandic rainwater is  $2.7 \times 10^{-5}$  mol/kg (Gislason et al., 1996). This value is less than 3% of that dissolved in the spring waters. Nevertheless, this annual  $\text{CO}_2$  discharge should only be taken as a minimum estimate. There are two other potentially significant  $\text{CO}_2$  discharge pathways to the surface in this system: (1)  $\text{CO}_2$  charged groundwater leaving the system through different rivers and (2)  $\text{CO}_2$  degassing from the groundwater through the lavas.

#### 4.1.3. Mobility of trace metals

Iron, Mn and Sr concentrations were measured in all ground water samples. Other trace element concentrations were measured in only the 12 samples collected in 2006 from the largest springs. These results are reported in the Appendix. The concentrations of Fe, Mn and Sr ranged from 6 to 115 nmol/kg, 0.42 to 11.7 nmol/kg and 117 to 407 nmol/kg, respectively. Most of the samples analyzed for Fe and Mn in the period 1988–1992 are below detection limits of the ICP-AES method used in this study. The concentrations of B, Ba, Co, Cr, Cu, Ni, Zn, Mo, Se, Li and V were low, slightly above the detection limits in more than half of the samples. The concentration of Cd, Pb and Hg together with As were below detection limits in most of the samples.

Moune et al. (2006) reported the concentrations of several trace elements in the Mt. Hekla 2000 lava. The concentrations were 11.26 wt% total Fe (expressed as FeO) and 46.3, 26.2, 211, 0.186, 344 and 3.25 ppm, respectively for Co, Cu, Zn, Cd, Ba and Pb. These values were used to calculate the relative mobility of these trace

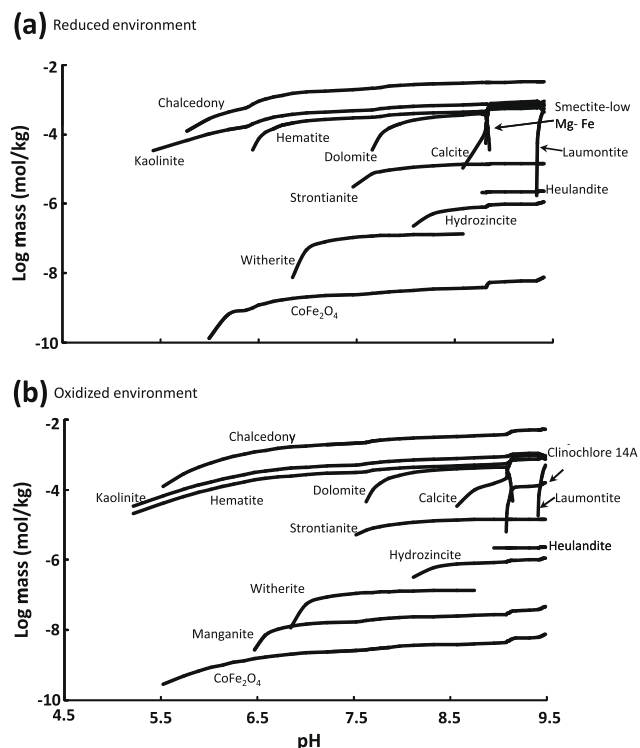
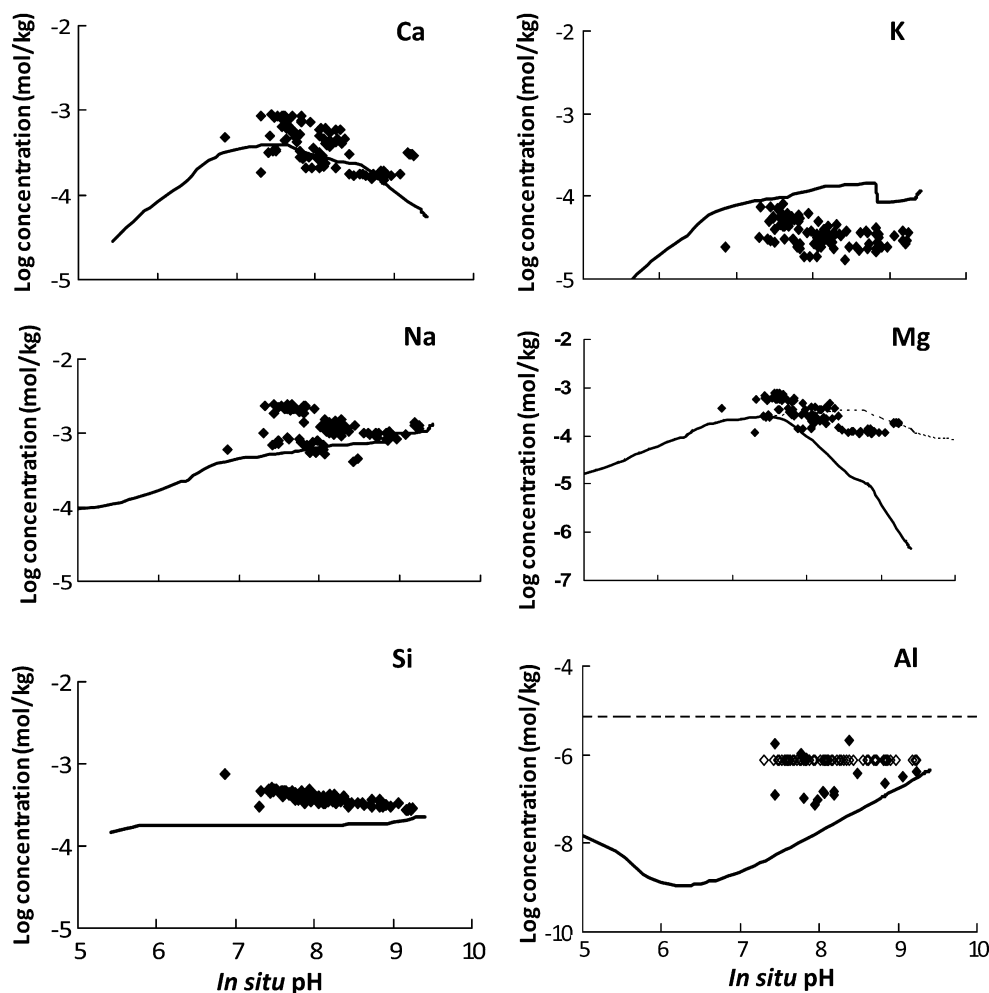


Fig. 7. Results of reaction path modelling. (a) Logarithm of the masses of secondary minerals precipitated during reaction path modelling for reduced environments. (b) Logarithm of the masses of secondary minerals precipitating during reaction path modelling for oxidized environments.



**Fig. 8.** A comparison of the concentration of major elements in the Hekla spring waters with those obtained by reaction path modelling. Closed symbols correspond to measured solution concentration and open symbols correspond to the maximum possible concentrations for samples below the detection limit. The solid curves represent the results of model calculations and the thin dotted line in the Mg diagram was obtained from reaction path modelling without allowing smectite and clinocllore to precipitate. The dotted line in the Al diagram is the drinking water guidelines given by the [European Community \(1998\)](#), and [WHO \(2006\)](#). The uncertainty in the analyses is approximated by the symbol size. 93 of 97 water samples collected between 1988 and 1992 had Al concentrations below the detection limit ( $7.4 \times 10^{-7}$  mol/kg).

metals shown in Fig. 4a. The sequence of relative mobility is  $\text{Cd} > \text{Cu} > \text{Zn} > \text{Ba} > \text{Al} > \text{Ti} > \text{Mn} > \text{Co} > \text{Fe}$ . This is roughly consistent with results from [Aiuppa et al. \(2000\)](#), who reported the mobility of trace elements from the Mt. Etna volcano. The mobility of these trace elements versus in situ pH is shown in Fig. 4b. Barium is the only metal which shows a clear trend; its mobility decreases with increasing pH.

#### 4.2. Saturation state ( $A_s$ ) of minerals and volcanic glasses in the spring waters

The saturation states of minerals and glasses are quantitative constraints on their tendency to dissolve or precipitate in the water. The saturation states of various mineral phases in the spring waters were calculated using the computer code PHREEQC 2.14.2 ([Parkhurst and Appelo, 1999](#)). Results are shown in Fig. 5 for the primary phase and in Fig. 6 for secondary minerals.

Because calcite is the most common carbonate mineral, insight into the ability of the Mt. Hekla system to sequester  $\text{CO}_2$  can be gained by considering the saturation state of Ca bearing solids. Hydrated Hekla 2000 glass is undersaturated in all the springs, as can be seen in Fig. 5, suggesting that the glass is an effective source for aqueous  $\text{Ca}^{2+}$  in this system. All primary minerals including anor-

thite, pyroxene and olivine are also undersaturated in the spring waters. Common secondary Ca-bearing phases in Iceland include carbonates, smectites and sometimes anhydrite ([Neuhoff et al., 1999](#); [Mehegan et al., 1982](#); [Kristmannsdóttir 1982](#); [Gislason et al., 1993](#)). The saturation indices of these minerals are shown in Fig. 6. The calculations show that smectites, laumontite and heulandite are saturated in all spring waters. Anhydrite and gypsum are highly undersaturated in the spring waters while calcite and dolomite are undersaturated at low pH but attain equilibrium in some springs at higher pH. These results suggest that although dolomite and calcite may form at elevated pH, providing mineralogical storage for dissolved  $\text{CO}_2$ , both clay minerals and zeolites can compete with carbonate minerals for  $\text{Ca}^{2+}$  ions, potentially limiting the Ca available for carbonate mineral precipitation. Other potential carbonate minerals including magnesite, siderite, cerussite, hydrozincite, rhodochrosite, otavite, strontianite, smithsonite and sphaerocobaltite are undersaturated in all the springs while witherite is saturated at high pH.

#### 4.3. Reaction path modelling

Reaction path modelling was performed using PHREEQC 2.14.2 ([Parkhurst and Appelo, 1999](#)) to simulate water–rock interaction in

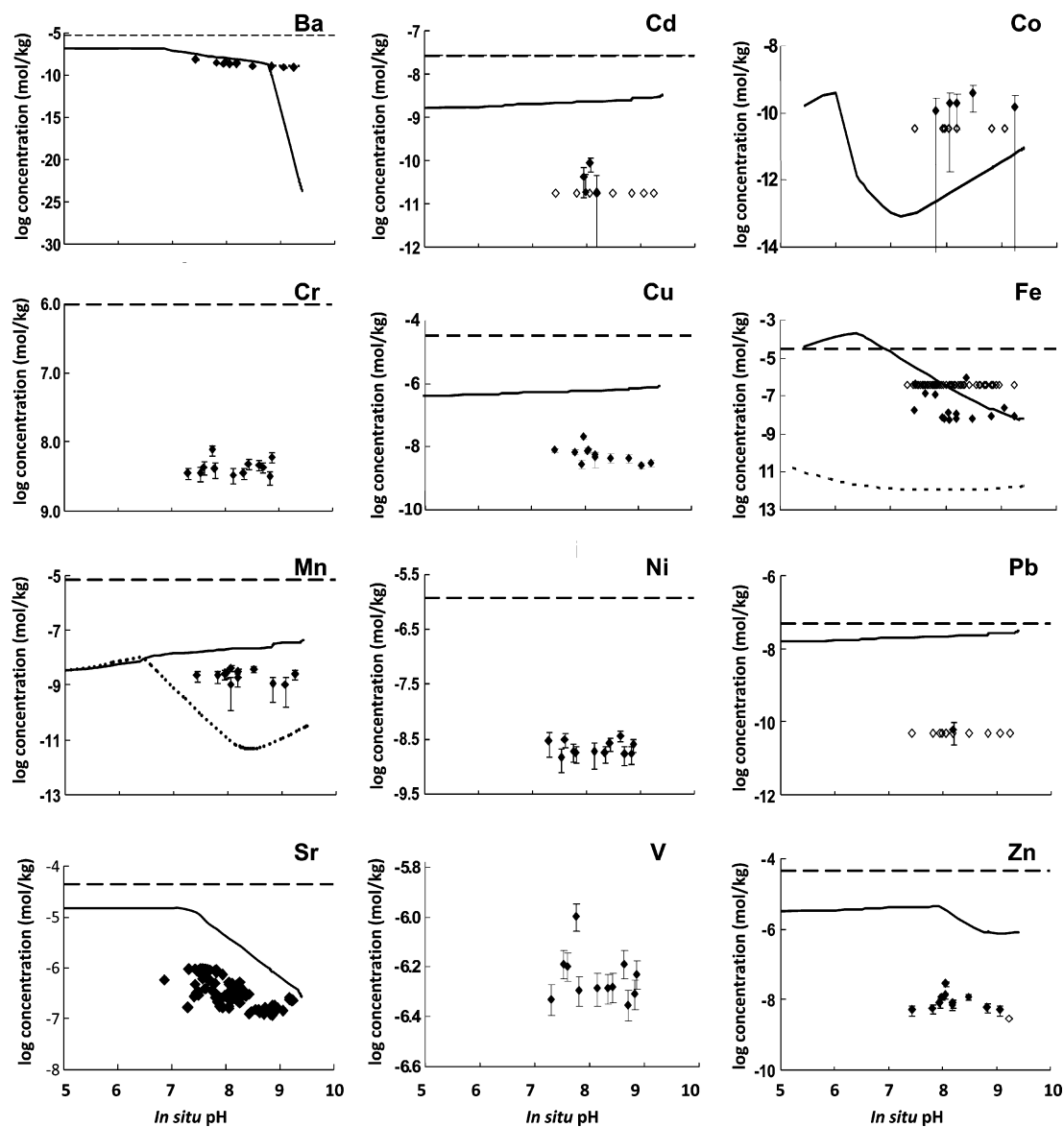


**Fig. 9.** Comparison between the trace element concentration of the Hekla spring waters with those obtained by reaction path modelling as a function of *in situ* pH. Closed symbols correspond to measured solution concentrations and open symbols correspond to the maximum possible concentrations for samples below the detection limit. The solid curves represent the results of reaction path modelling for reduced conditions and the dotted lines show the drinking water limits recommended by the European Community (1998), and WHO (2006). The thin dotted curve in the Ba diagram that fits all the samples including the three samples at the highest pH shows the concentration of Ba during reaction path modelling without heulandite precipitation. The thin dotted curve in the Fe and Mn diagrams stems from reaction path modelling during oxidized conditions (see text). When the errors bars are smaller than the symbol, the error bars are not shown.

the Hekla system. The modelling was performed under both reducing and oxidizing conditions. The  $O_2$  fugacity in the reducing environment was set by  $Fe^{2+}/Fe^{3+}$  equilibrium fixed by the dissolving basalt coupled to hematite precipitation; that of the oxidizing environment was set by assuming the solution was constantly in equilibrium with atmospheric  $O_2$ . The groundwater initially had a 0.05 bar  $CO_2$  partial pressure and  $pH = 4.5$ . As this solution reacts with Hekla glass, the  $pH$  increases and becomes supersaturated with respect to a number of secondary phases. The maximum  $pH$  attained during the modelling was 9.4. Within the model, secondary phases are assumed to precipitate and be in equilibrium with the fluid phase. The amount of the secondary minerals formed during the reaction path models are shown in Fig. 7. Modelling results for the reduced environment, illustrated in Fig. 7a, suggest that kaolinite is the first secondary mineral to precipitate at  $pH > 5.4$ . The oxides, chalcidony and  $CoFe_2O_4$  reach saturation at  $pH > 5.8$

and 6.0. Hematite attains saturation when  $pH$  reaches 6.3, and the carbonates, witherite, strontianite, dolomite and calcite attain saturation at  $pH > 6.8$ , 7.5, 7.7 and 8.6, respectively. Smectite precipitation begins at  $pH > 8.8$ . The zeolites heulandite and laumontite, attain saturation at  $pH$  8.8 and 9.3, respectively. These modelling calculations suggest that the major alteration phases are chalcidony, kaolinite and hematite at  $5.4 < pH < 8.0$ . At higher  $pH$  calcite, smectite, and eventually laumontite become important alteration phases. These results match the field observations reported by Kristmannsdóttir (1982), Mehegan et al. (1982), Neuhoff et al. (1999), which validates, in part, the model calculations. Model results for the oxidized system are shown in Fig. 7b. These results are similar to those of the reduced system other than (1) manganite, a mineral containing oxidized Mn is calculated to precipitate at  $pH > 6.5$ , and (2) clinocllore rather than smectite is calculated to precipitate at  $pH > 9$ . This latter result may be due to

lack of provision for solid-solutions in the thermodynamic database. The low  $\text{Fe}^{2+}$  concentration of the oxidized fluids destabilizes the  $\text{Fe}^{2+}$  bearing smectite in the model calculation.

## 5. Discussion

### 5.1. Controls on major element mobility

Insight into metal mobility can be obtained from the results of reaction path modelling. The concentrations of major elements in the springs are compared with those from the reaction path modelling in Fig. 8. As can be seen in Fig. 8, the concentrations of major elements tend to be close to those estimated from the model calculation. In some cases however, there are important differences between model calculations and spring water concentrations. For example, spring water Si concentrations are systematically higher than the model values. This suggests that the precipitation kinetics of chalcedony, which is the commonly observed  $\text{SiO}_2$  phase in altered basalts, are sluggish. This observation is consistent with the results of Rogers et al. (2006), who reported that amorphous silica is the common silica phase formed via the low-temperature alteration of basalts by  $\text{CO}_2$ -rich fluids. Similar sluggish kinetics or the affect of allophane precipitation may be responsible for the scatter observed among the spring water Al concentrations. Note that allophane was not present in the thermodynamic database. Spring water Mg concentrations are significantly higher at  $\text{pH} > 7.5$  than the modelled counterparts. This may be due to sluggish smectite and clinocllore precipitation kinetics; both of these minerals appear to be significantly supersaturated in the Hekla spring waters at this pH (see Fig. 6). By removing smectite and clinocllore precipitation from the reaction path model, the modelled Mg concentrations are equal to the spring water concentrations as can be seen in Fig. 8. Another factor that could lead to the underestimation of aqueous Mg concentrations in the model calculations is either sluggish dolomite kinetics or an overestimate of the stability of dolomite in the thermodynamic database. This possibility is suggested by the observation that, according to thermodynamic calculations, dolomite is supersaturated in many of the high pH spring waters (see Fig. 6). If dolomite was not allowed to precipitate in the reaction path modelling, the calculated quantity of calcite increased substantially.

### 5.2. Possible mobilization of toxic metals in groundwaters during $\text{CO}_2$ sequestration in basalt

The possible mobilization of toxic metals during injection of  $\text{CO}_2$  rich water into basalt poses a potential risk for  $\text{CO}_2$  sequestration in these rocks. The results presented above illuminate the limits on potential toxic metal mobility stemming from  $\text{CO}_2$ -basalt interaction. The concentrations of trace metals are very low in the spring waters, with concentrations ranging from  $10^{-6}$  to  $10^{-11}$  mol/kg (see Fig. 9). These concentrations are all below the drinking water guidelines given by the WHO (2006) and the European Community (1998). The degree to which measured spring water trace metal concentrations correspond to those generated from model calculations depends on the identity of the metal and are shown in Fig. 9. Barium spring water concentrations closely match those of model calculations at  $\text{pH} < 9$ . At this pH, aqueous Ba concentrations in the model calculations are controlled by witherite solubility. At higher pH, the modelled aqueous Ba concentration decreases rapidly with increasing pH due to heulandite precipitation. This decrease is not, however, reflected in the spring water concentration, and may be an artefact of the chemical composition of the heulandite present in the thermodynamic database. Spring water Co concentrations are significantly greater than their modelled counterparts. As Co concentrations in the model calculations

are controlled by  $\text{CoFe}_2\text{O}_4$  precipitation and the observation that the Hekla spring waters are highly supersaturated with respect to this phase it seems likely that  $\text{CoFe}_2\text{O}_4$  does not precipitate in the natural system. Cobalt could, however, be incorporated in oxyhydroxides (as  $\text{Co}(\text{OH})_3$ ), as suggested by Marini et al. (2001). The modelled concentrations of Fe for the reduced conditions closely match those of the spring samples. In the reduced model calculation, Fe is controlled by hematite solubility. According to Stefánsson and Gislason (2001), surface waters in Iceland are close to saturation with amorphous  $\text{FeOOH}$ . Arnalds et al. (1995) identified three clay size phases in Icelandic soils: allophane, imogolite and poorly crystalline ferrihydrite. These phases are mostly amorphous to X-rays. In the model calculations, hematite appears in this calculation rather than either amorphous  $\text{FeOOH}$  or ferrihydrite because hematite is more stable. The corresponding calculation for the oxidized environment yields estimates of Fe and Mn concentrations that are far below those measured in the spring waters. This suggests that the redox state of the Hekla area groundwater is somewhat reduced and buffered by Fe(II) in the volcanic glass. Spring water Cu, Cd, Zn, Pb and Sr concentrations are far less than those estimated from the reaction path calculations, yet the calculations suggest that all Cu, Cd, Zn, Pb and Sr bearing solid phases are undersaturated except for hydrozincite at  $\text{pH} > 8.0$ . The reason for the large difference between certain trace metals in the model calculations and the spring water concentrations may stem from the adsorption of these metals on the surface of the precipitated secondary phases; such adsorption is not accounted for in the model. Iron(III) and Al(III) oxides are often used as coagulants in water and soil treatments because of their scavenging properties (Stumm and Morgan, 1996; Jackson and Bistricki, 1995; Kumpiene et al., 2008; Fatoki and Ogunfowokan, 2002). They readily scavenge metals like Cr, Ni, Cd, Mn, Zn and to a lesser extent Cu and As. The degree of scavenging normally increases with increasing pH (Fatoki and Ogunfowokan, 2002). Strontium is known to co-precipitate with aragonite, but thermodynamic data for the solid-solution of orthorhombic carbonates is not present in the model. The large

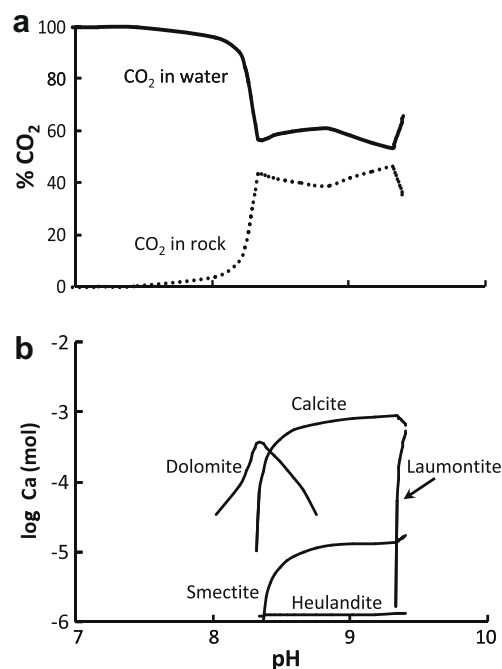


Fig. 10. (a) The distribution of inorganic C in the system between the aqueous and solid phase during the reaction path modelling. (b) The distribution of  $\text{Ca}^{2+}$  among secondary minerals forming during reaction path modelling.

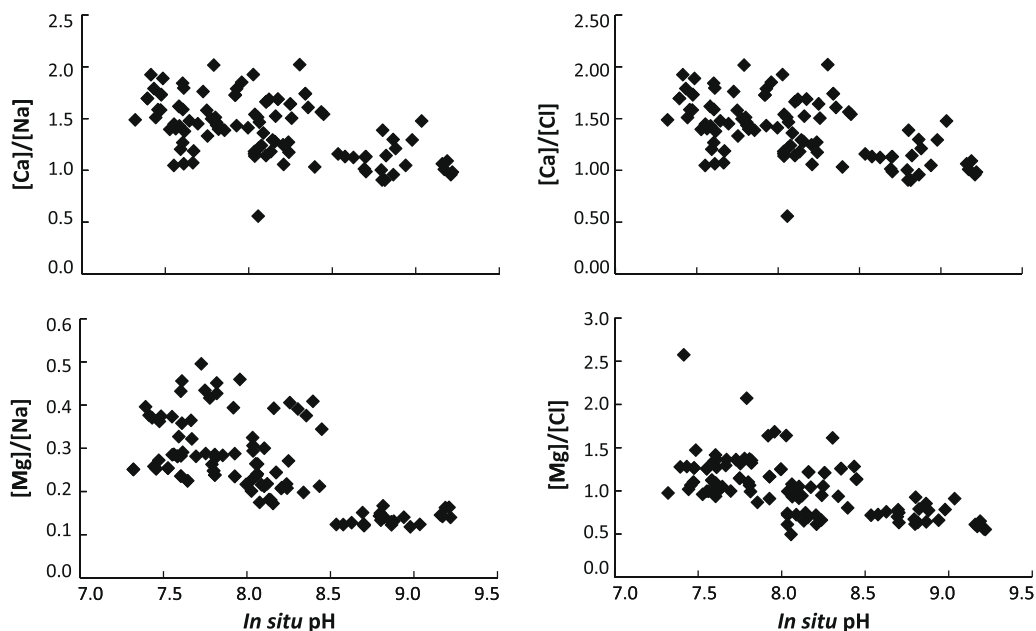


Fig. 11. Spring water Ca/Na, Mg/Na, Ca/Cl and Mg/Cl concentration ratios plotted as a function of *in situ* pH.

differences between measured and modelled trace metal concentrations illustrate the current limitations in quantifying trace element mobility using currently available thermodynamic databases.

### 5.3. CO<sub>2</sub> fixation in the Mt. Hekla ground water system

The variation of spring water DIC concentrations with pH, as illustrated in Fig. 3b, suggests that basalt–fluid interaction can fix dissolved CO<sub>2</sub> as carbonate minerals. Further insight into this process can be gained through the aid of Fig. 10. Fig. 10a shows the relative amount of C in the aqueous versus secondary minerals according to the model calculation, as a function of pH. At low pH, all C is present in the aqueous phase. When pH exceeds 7.7, dolomite precipitates fixing CO<sub>2</sub> into the solid phase followed by calcite at pH 8.6. The amount of calcite precipitation increases until pH 9.3 when 43% of all CO<sub>2</sub> is fixed in the solid. This result is roughly consistent with the field data shown in Fig. 4b where a pH increase from 7 to 9 decreases DIC concentration by roughly a factor of three. When the pH increases further in the model calculation, however, calcite dissolves and the amount of CO<sub>2</sub> in the water phase increases. The origin of this high pH behaviour can be deduced by considering Fig. 10b, which shows the distribution of Ca among the precipitated mineral phases. The first Ca-bearing mineral to attain saturation is dolomite followed by calcite, heulandite, smectite and laumontite. Since the amount of Ca consumed by smectite and heulandite formation is relatively small compared to calcite, they do not strongly affect the amount of calcite precipitating. In contrast, laumontite competes with calcite for Ca, limiting CO<sub>2</sub> fixation in the reaction path calculation at pH > 9.3. The consumption of divalent metal cations by carbonate precipitation during fluid–basalt interaction is also suggested by the measured source water compositions. The source water Ca/Na, Mg/Na, Ca/Cl and Mg/Cl concentration ratios are plotted as a function of pH in Fig. 11. Aqueous Ca and Mg concentrations decrease more strongly with pH than Na and Cl, consistent with both the reaction path calculations and the incorporation of these metals in precipitated carbonate minerals.

Further insight into the potential for CO<sub>2</sub> fixation as carbonate minerals in basaltic rocks can be attained by performing similar reaction path calculations for initial fluids containing higher CO<sub>2</sub>

pressures. Such calculations have previously been presented by Marini (2007), Gysi and Stefánsson (2008).

## 6. Conclusions

The results presented above illuminate the fate of both CO<sub>2</sub> and dissolved metals during the interaction of CO<sub>2</sub>-rich rainwater and basaltic rocks. The major conclusions of this study include:

1. Results indicate that the neutralization of CO<sub>2</sub>-rich waters by their interactions with basalt in the subsurface may provide an effective means to fix CO<sub>2</sub> as carbonate minerals. This process proceeds by the combination of Ca and Mg liberated to solution through basalt dissolution driven by dissolved CO<sub>2</sub> to form calcite and perhaps dolomite. This process may be limited, however, by competition for dissolved Ca between precipitating carbonates and Ca-bearing aluminosilicate secondary phases such as zeolites and smectites.
2. Toxic metal mobility is limited during the movement of CO<sub>2</sub>-rich water through basaltic rock. Reaction path calculations suggest that although these metals may be liberated by the initial dissolution of basalt in acidic CO<sub>2</sub> rich waters, these metals are incorporated, at least partly, in precipitating carbonates and Fe(III) (oxy)hydroxides as the fluid phase is neutralized by further basalt dissolution.

## Acknowledgements

We thank Luigi Marini and Stefano Caliro for constructive reviews that led to significant improvements of the manuscript. We are grateful to many friends and colleagues for their help. Specifically we would like to thank Guðmundur B. Ingvarsson for helpful discussions and Rósa Ólafsdóttir for assisting with GIS. We would also like to thank the Carb-Fix consortium; Wallace S. Broecker, Juerg M. Matter, Hólmfríður Sigurðardóttir, Andri Stefánsson, Domenik Wolff-Boenisch, Einar Gunnlaugsson, Grímur Björnsson, Alexander Gysi, Edda Sif Aradóttir, Gabrielle J. Stockmann, Helgi Arnar Alfredsson and Snorri Gudbrandsson. This study was supported by The Nordic Volcanological Institute Fellowship, the

Science Institute of the University of Iceland and the MIN-GRO Research and Training Network (MRTN-CT-2006-035488).

## Appendix A. Supplementary data

Supplementary data associated with this article can be found, in the online version, at doi:10.1016/j.apgeochem.2008.12.031.

## References

- Aiuppa, A., Allard, P., D'Alessandro, W., Michel, A., Parello, F., Treuil, M., Valenza, M., 2000. Mobility and fluxes of major, minor and trace metals during basalt weathering and groundwater transport at Mt. Etna volcano (Sicily). *Geochim. Cosmochim. Acta* 64, 1827–1841.
- Aiuppa, A., Caleca, A., Federico, C., Gurreri, S., Valenza, M., 2004. Diffuse degassing of carbon dioxide at Somma-Vesuvius volcanic complex (southern Italy) and its relation to regional tectonics. *J. Volc. Geothermal Res.* 133, 55–79.
- Allard, P., Carbonelle, J., Dajlevic, D., Le Bronec, J., Morel, P., Robe, M.C., Maurenas, J.M., Faivre-Pierret, R., Martin, D., Sabroux, J.C., Zettwoog, P., 1991. Eruptive and diffusive emissions of CO<sub>2</sub> from Mount Etna. *Nature* 351, 387–391.
- Arnalds, O., Hallmark, C.T., Wilding, L.P., 1995. Andisols from four different regions of Iceland. *Soil. Sci. Soc. Am. J.* 59, 161–169.
- Árnason, B., 1976. Groundwater systems in Iceland traced by deuterium. *Reykjavík, Societas Scientiarum Islandica*.
- Brady, P.V., Gislason, S.R., 1997. Seafloor weathering controls on atmospheric CO<sub>2</sub> and global climate. *Geochim. Cosmochim. Acta* 61, 965–973.
- Craig, H., 1961. Isotopic variations in meteoric waters. *Science* 133, 1702–1703.
- European Community, 1998. Council directive 98/83 Official Journal of the European Community.
- Fatoki, O.D., Ogunfowokan, A.O., 2002. Effect of coagulant treatment on the metal composition of raw water. *Water SA* 28, 293–298.
- Federico, C., Aiuppa, A., Bellomo, S., Jean-Baptiste, P., Parello, Valenza M., 2002. Magma-derived gas influx and water–rock interactions in the volcanic aquifer of Mt. Vesuvius, Italy. *Geochim. Cosmochim. Acta* 66, 963–981.
- Flaathen, T.K., Gislason, S.R., 2007. The effect of volcanic eruptions on the chemistry of surface waters: the 1991 and 2000 eruptions of Mt. Hekla, Iceland. *J. Volc. Geothermal Res.* 164, 293–316.
- Gaillardet, J., Dupré, B., Allègre, C.J., 1999. Global silicate weathering and CO<sub>2</sub> consumption rates deduced from the chemistry of large rivers. *Chem. Geol.* 159, 3–30.
- Gislason, S.R., Arnórsson, S., 1990. Saturation state of natural waters in Iceland relative to primary and secondary minerals in basalts I. In: Spencer, R.J., I-Ming Chou (Eds.), *Fluid–Mineral Interactions: a Tribute to H.P. Eugster*. Geochemical Society, Special Publication No. 2, pp. 373–393.
- Gislason, S.R., Arnórsson, S., 1993. Dissolution of primary basaltic minerals in natural waters: saturation state and kinetics. *Chem. Geol.* 105, 117–135.
- Gislason, S.R., Oelkers, E., 2003. Mechanism, rates, and consequences of basaltic glass dissolution; II. An experimental study of the dissolution rates of basaltic glass as a function of pH and temperature. *Geochim. Cosmochim. Acta* 67, 3817–3832.
- Gislason, S.R., Andrésdóttir, A., Sveinbjörnsdóttir, Á.E., Óskarsson, N., Thordarson, Th., Torssander, P., Novák, M., Zák, K., 1992. Local effects of volcanoes on the hydrosphere: example from Hekla, southern Iceland. In: Kharaka, Y.K., Maest, A.S. (Eds.), *Water–Rock Interaction*. Balkema, Rotterdam, pp. 477–480.
- Gislason, S.R., Arnórsson, S., Ármannsson, H., 1996. Chemical weathering of basalt in southwest Iceland: effect of runoff, age of rocks and vegetative/glacial cover. *Am. J. Sci.* 296, 837–907.
- Gislason, S.R., Gunnlaugsson, E., Broecker, W.S., Oelkers, E.H., Matter, J.M., Stefánsson, A., Arnórsson, S., Björnsson, G., Fridriksson, T., Lackner, K., 2007. Permanent CO<sub>2</sub> sequestration into basalt: the Hellisheidi, Iceland project. *Geophys. Res. Abstr.* 9, 07153.
- Gislason, S.R., Snorrason, Á., Eiríksdóttir, E.S., Sigfússon, B., Elefsen, S.O., Harðardóttir, J., Gunnarsson, Á., Torssander, P., 2003. Chemical composition, discharge and suspended material in rivers in South-Iceland, VI. Database of Science Institute and National Energy Authority. Science Institute, RH-03-2003 (in Icelandic).
- Gislason, S.R., Stefánsson, Á., Eiríksdóttir, E.S., 2000. ARCTIS, Regional Investigation of Arctic Snow Chemistry: Results from the Icelandic Expeditions, 1997–1999. *Raunvísindastofnun, RH-05-2000*.
- Gislason, S.R., Veblen, D.R., Livi, K.J.T., 1993. Experimental meteoric water–basalt interactions: characterization and interpretation of alteration products. *Geochim. Cosmochim. Acta* 57, 1459–1471.
- Gronvold, K., Larsen, G., Einarsson, P., Thorarinnsson, S., Saemundsson, K., 1983. The Hekla eruption 1980–1981. *Bull. Volcanol* 46, 349–363.
- Gudmundsson, A., Óskarsson, N., Gronvold, K., Saemundsson, K., Sigurdsson, O., Stefánsson, R., Gislason, S.R., Einarsson, P., Brandsdóttir, B., Larsen, G., Johannesson, H., Thordarson, T., 1992. The 1991 eruption of Hekla, Iceland. *Bull. Volcanol.* 54, 238–246.
- Gysi, A.P., Stefánsson, A., 2008. Numerical modelling of CO<sub>2</sub>–water–basalt interaction. *Mineral. Mag.* 72, 55–59.
- Intergovernmental Panel on Climate Change, 2005. *Carbon dioxide capture and storage*. Cambridge University Press, New York.
- Jackson, A.J., Bistricki, T., 1995. Selective scavenging of copper, zinc, lead and arsenic by iron and manganese oxyhydroxide coatings on plankton in lakes polluted with mine and smelter wastes: results of energy dispersive X-ray microanalysis. *J. Geochem. Explor.* 52, 97–125.
- Kjartansson, G., 1957. Some secondary effects of the Hekla eruption. Exhalations of carbon dioxide, contamination of ground-water and lowering of water table. In: Einarsson, T., Kjartansson, G., Þorarinsson, S. (Eds.), *The Eruption of Hekla 1947–1948 III*. Societas Scientiarum Islandica.
- Kristmannsdóttir, H., 1982. Alteration in the IRDP Drill Hole compared with other drill holes in Iceland. *J. Geophys. Res.* 87, 6525–6531.
- Kumpiene, J., Lagerkvist, A., Maurice, C., 2008. Stabilization of As, Cr, Cu, Pb and Zn in soil using amendments – a review. *Waste Manage.* 28, 215–225.
- Marini, L., 2007. *Geological Sequestration of Carbon-dioxide: Thermodynamics, Kinetics and Reaction Path Modeling*. Elsevier, Amsterdam.
- Marini, L., Canepa, M., Cipolli, F., Ottonello, G., Zuccolini, M.V., 2001. Use of stream sediment chemistry to predict trace element chemistry of groundwater. A case study from the Bisagno valley (Genoa, Italy). *J. Hydrol.* 241, 194–220.
- Matter, J.M., Takahashi, T., Goldberg, D., 2007. Experimental evaluation of in situ CO<sub>2</sub>–water–rock reactions during CO<sub>2</sub> injection in basaltic rocks: implications for geological CO<sub>2</sub> sequestration. *Geochim. Geophys. Geosys.* 8, doi: 10.1029/2006GC001427.
- McGrail, B.P., Schaefer, H.T., Ho, A.M., Chien, Y.J., Dooley, J., 2006. Potential for carbon dioxide sequestration in flood basalts. *J. Geophys. Res.* 111, B12201. doi:10.1029/2005JB004169.
- Mehegan, J.M., Robinson, P.T., Delaney, J.R., 1982. Secondary mineralization and hydrothermal alteration in the Reydarfjörður drill core, Eastern Iceland. *J. Geophys. Res.* 87, 6511–6524.
- Moune, S., Gauthier, P.-J., Gislason, S.R., Sigmarsson, O., 2006. Trace elements degassing and enrichment in the eruptive plume of the 2000 eruption of Hekla volcano, Iceland. *Geochim. Cosmochim. Acta* 70, 461–479.
- Neuhoff, P.S., Fridriksson, T., Arnórsson, S., Bird, D.K., 1999. Porosity evolution and mineral paragenesis during low-grade metamorphism of basaltic lavas at Teighathorn, Eastern Iceland. *Am. J. Sci.* 299, 467–501.
- Oelkers, E.H., Cole, D.R., 2008. Carbon dioxide sequestration: a solution to a global problem. *Elements* 4, 305–310.
- Oelkers, E.H., Schott, J., 2005. *Geochemical Aspects of CO<sub>2</sub> sequestration*. *Chem. Geol.* 217, 183–186.
- Oelkers, E.H., Gislason, S.R., Matter, J., 2008. Mineral carbonation of CO<sub>2</sub>. *Elements* 4, 333–337.
- Parkhurst, D.L., Appelo, C.A.J., 1999. *User's guide to PHREEQC (Version 2) – A computer program for speciation, batch-reaction, one-dimensional transport, and inverse geochemical calculations*. U.S. Geol. Surv. Water Invest. Rep. 99-4259.
- Rogers, K.L., Neuhoff, P.S., Pedersen, A.K., Bird, D.K., 2006. CO<sub>2</sub> metasomatism in a basalt hosted petroleum reservoir, Nuussuaq, West Greenland. *Lithos* 92, 55–82.
- Sigvaldason, G.E., 1974. The eruption of Hekla 1947/1948. The petrology of Hekla and origin of silicic rocks in Iceland. In: Einarsson, T., Kjartansson, G., Þorarinsson, S. (Eds.), *The Eruption of Hekla 1947-1948 V*. Societas Scientiarum Islandica.
- Stefánsson, A., Gislason, S.R., 2001. Chemical weathering of basalts, southwest Iceland: effect of rock crystallinity and secondary minerals on chemical fluxes to the ocean. *Am. J. Sci.* 301, 513–556.
- Stumm, W., Morgan, J.J., 1996. *Aquatic Chemistry, Chemical Equilibria and Rates in Natural Waters*. Wiley, Interscience publication, New York.
- Walker, J.C.G., Hays, P.B., 1981. A negative feedback mechanism for the long-term stabilization of Earth's surface temperature. *J. Geophys. Res.* 86, 9776–9782.
- WHO, 2006. *Guidelines for Drinking-water Quality*, 3rd ed., incorporating first addendum.
- Wolff-Boenisch, D., Gislason, S.R., Oelkers, E.H., 2006. The effect of crystallinity on dissolution rates and CO<sub>2</sub> consumption capacity of silicates. *Geochim. Cosmochim. Acta* 70, 858–870.
- Wolff-Boenisch, D., Gislason, S.R., Oelkers, E.H., Putnis, C.V., 2004. The dissolution rates of natural glasses as a function of their composition at pH 4 and 10.6, and temperatures from 25 to 74 °C. *Geochim. Cosmochim. Acta* 68, 4843–4858.